Dynamics of Coupled Nonlinear Oscillators and Multiplex Networks of Logistic Maps

AMOL AMODKAR

A dissertation submitted for the partial fulfillment
of BS-MS (dual-degree) in Science

Indian Institute of Science Education and Research (IISER) Mohali, India
April 2018

Certificate of Examination

This is to certify that the dissertation titled **Dynamics of Coupled Nonlinear Oscillators and Multiplex Networks of Logistic Maps** submitted by **Amol Madhukar Amodkar** (Reg. No. MS13052) for the partial fulfilment of BS-MS dual degree program of Indian Institute of Science Education and Research (IISER) Mohali, has been examined by the committee duly appointed by the Institute. The committee finds the work done by the candidate satisfactory and recommends that the report is accepted.

Dr. Chandrakant Aribam	Dr. Abhishek Chaudhuri	Prof. Sudeshna Sinha
		(Thesis Guide)

Dated: April 20, 2018

Declaration

The work presented in this dissertation has been carried out by me under the guidance of Prof. Sudeshna Sinha at the Indian Institute of Science Education and Research Mohali.

This work has not been submitted in part or in full for a degree, a diploma, or a fellowship to any other university or institute. Whenever contributions of others are involved, every effort is made to indicate this clearly, with due acknowledgement of collaborative research and discussions. This thesis is a bonafide record of original work done by me and all sources listed within have been detailed in the bibliography.

Amol Madhukar Amodkar

(Candidate)

Dated: April 20, 2018

In my capacity as the MS thesis supervisor of the candidate, I certify that the above statements by the candidate are true to the best of my knowledge.

Prof. Sudeshna Sinha
(Supervisor)

Acknowledgements

I would like to express my sincere gratitude to my thesis supervisor, Prof.Sudeshna Sinha, for giving me an opportunity to work under her guidance and for constant support and encouragement throughout my work. I would like to thank Dr Chandrakant Aribam and Dr Abhishek Chaudhuri for their valuable feedback and for evaluating my work.

I would also like to thank IISER Mohali for giving me an opportunity and providing excellent facilities.

Finally, I thanks my friends and family members for constant support and encouragement and to bear with me during this journey.

List of Figures

Contents

Abstract

In this thesis, we studied some basic properties of dynamical systems in the first chapter, in particular, Linear Stability analysis which provides a framework to understand the stability of a dynamical system in the neighborhood of fixed points.

In the second chapter, we apply the Linear stability formalism to a general system coupled by mean-field diffusive coupling. We then use the framework to analyze the steady state of groups of Landau Stuart(LS) Oscillators coupled via a common environment. We obtain the different steady-state solutions of the LS Oscillator in the parameter space of the oscillator-environment coupling strength.

In the third chapter, we study the multiplex network. Our main emphasis was on the intra-layer and inter-layer synchronization and to understand the effect of various parameters on the synchronization region. We considered the prototypical logistic map at the nodes of both layers of the multiplex network. Further, we study the emergent dynamics under parameter mismatch in the layers of the multiplex network.

Chapter 1

Introduction

1.1 Linear Stability Analysis

First, we consider a one-dimensional flow, given by the differential equation $\dot{x} = f(x)$. When $f(x^*) = 0$, x^* is a *fixed point(s)* [14] Now, fixed points can be classified into two principal types:

- Stable fixed points: these are fixed points in which sufficiently small disturbances around the fixed point decay with time.
- Unstable fixed points: these are fixed points in which small disturbances around the fixed point grow in time.

We would like to have a more quantitative measure of stability, such as a rate of decay or growth to a fixed point. We can get such information by linearizing about a fixed point as follows.

Let x^* be a fixed point and $\eta(t) = x(t) - x^*$ be a small perturbation away from x^*. Differentiating yields,

$$\eta' = x' + 0 = x' \tag{1.1}$$

as x^* is constant.Now, $\eta' = x' = f(x) = f(x^* + \eta)$. Using, Taylor series expansion we get,

$$f(x^* + \eta) = f(x^*) + \eta \times f'(x^*) + O(\eta^2) \tag{1.2}$$

where $O(\eta^2)$ denotes quadratically small terms in η and $f'(x^*) = 0$ since x^* is a fixed point. Considering $O(\eta^2)$ terms to be negligible, we obtain the following:

$$\eta' \approx \eta \times f'(x^*) \tag{1.3}$$

This is the linear equation in η and called a linearization about x^* [14]. Now perturbation $\eta(t)$ grows *exponentially* if $f'(x^*) > 0$ and decays if $f'(x^*) < 0$. So in the former case, x^* is an **unstable** fixed point and in latter case it is a **stable** fixed point.

For a 2-dimensional flow given by $\dot{\mathbf{x}} = \mathbf{f}(\mathbf{x})$, with $\mathbf{x}$ having two components, a detailed analysis of the fixed points can be seen in 1.1.

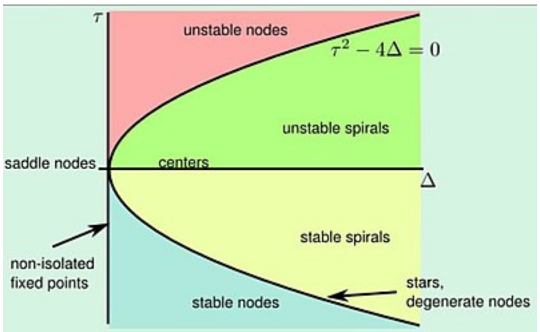

Figure 1.1: Stability of fixed points

Here, τ and Δ denotes the trace and determinant of the Jacobian matrix of $\mathbf{f}(\mathbf{x})$ respectively. We can observe the following from the figure:

- If $\Delta < 0$, the eigenvalues are real and have opposite signs,then the fixed point is a saddle [14]
- If $\Delta > 0$, the eigenvalues are either real with same signs(nodes), or complex conjugate (spirals and centers) [14].
- When $\tau < 0$, eigenvalues have negative real part, so the fixed point is stable [14].

So, for a fixed point to be **stable** $Re(\lambda) < 0$ for all eigenvalues.

1.2 Bifurcation

The qualitative structure of the flow can be changed as parameters are varied. In particular, fixed points can be created or destroyed by changing the parameters. These qualitative changes are called *bifurcations*, and the parameters values at which they occur are called *bifurcation points* [14].

1.2.1 Saddle-Node Bifurcation

The saddle-node is the bifurcation in which fixed points are created and destroyed. As a parameter is varied, two fixed points move toward each other, collide and then disappears [14].

Example:

$$\dot{x} = r + x^2 \tag{1.4}$$

where r is a parameter. If we plot x versus $\dot{x}$ then we get a parabola which depends on the value of r. If $r < 0$ then there will be two fixed points. As r approaches 0, two fixed points start to move towards each other and at $r = 0$ we get only one fixed point and as becomes $r > 0$ the fixed points disappear.

Stability of the fixed points can be checked by linearisation method. So, $f(x) = 0$ gives $r = -x^2$ and at all the points where $f'(x^*) < 0$ will be stable points and vice-versa.

1.2.2 Transcritical Bifurcation

In transcritical bifurcation, fixed points must exist for all the values of a parameter and can never be destroyed. So, as a parameter is varied the stability of a fixed point changes.[14]
The normal form of a transcritical bifurcation is

$$\dot{x} = rx - x^2 \tag{1.5}$$

So, for these equation $x^* = 0$ is a fixed point for all values of r. When $r < 0$, $x^* = 0$ is a stable fixed point and at $r = 0$ it changes to half-stable and as soon as $r > 0$ it becomes unstable.

1.2.3 Pitchfork Bifurcation

This bifurcation is common in physical systems having *symmetry*. In such cases, fixed points tend to appear and disappear in symmetrical pairs [14].

There are two types of Pitchfork Bifurcation, which we describe below.

Supercritical Pitchfork Bifurcation

The normal form of the supercritical pitchfork bifurcation is

$$\dot{x} = rx - x^3 \tag{1.6}$$

This equation is *invariant* under the change of variable $x \to -x$ which indicates left-right symmetry.
As we can see from the equation that when $r \leq 0$, an origin is the only fixed point and when $r > 0$ two stable fixed points appear on either side symmetrically and origin becomes unstable.

Critical Slowing down

When $r = 0$, the origin is stable, but the solution no longer decays exponentially fast as it was in the case when r was less than 0. Instead, the decay is a much slower function of time. This lethargic decay is called *critical slowing down* [14].

Sub-critical Pitchfork Bifurcation

The normal form of the sub-critical pitchfork bifurcation is

$$\dot{x} = rx + x^3 \tag{1.7}$$

In the supercritical case, $-x^3$ was stabilizing, but here x^3 is the destabilizing term. So, if there is any small perturbation, then the cubic term will help in driving trajectories to infinity.
In this case, the fixed points will appear when $r < 0$ and will be unstable and origin will become stable when $r < 0$.

1.3 Linearization

In this section, we will extend the technique of linear stability to the higher dimension systems.
Consider the following set of an autonomous system:

$$\dot{\mathbf{x}} = \mathbf{f}(\mathbf{x}) \tag{1.8}$$

and let $\mathbf{x}^*$ be the fixed point of the system.
By definition, $\mathbf{f(x^*)}$=0.
Let's take the Taylor expansion of the right-hand side of the equation (1.8).

$$\begin{aligned} \dot{\mathbf{x}} &= \mathbf{f}(\mathbf{x}^*) + \left.\frac{\partial \mathbf{f}}{\partial \mathbf{x}}\right|_{\mathbf{x}^*} (\mathbf{x} - \mathbf{x}^*) + \cdots \\ &= \left.\frac{\partial \mathbf{f}}{\partial \mathbf{x}}\right|_{\mathbf{x}^*} (\mathbf{x} - \mathbf{x}^*) + \cdots \end{aligned} \tag{1.9}$$

The partial derivatives in (1.9) can be interpreted as the Jacobian Matrix, if the components of the state vector $\mathbf{x}$ are $(x_1, x_2, \cdots, x_n)$ and the components of the rate vector $\mathbf{f}$ are $(f_1, f_2, \cdots, f_n)$ then the Jacobian matrix will be:

$$\mathbf{J}= \begin{bmatrix} \frac{\partial f_1}{\partial x_1} & \frac{\partial f_1}{\partial x_2} & \cdots & \frac{\partial f_1}{\partial x_n} \\ \frac{\partial f_2}{\partial x_1} & \frac{\partial f_2}{\partial x_2}s & \cdots & \frac{\partial f_2}{\partial x_n} \\ \vdots & \vdots & \cdots & \vdots \\ \frac{\partial f_n}{\partial x_1} & \frac{\partial f_n}{\partial x_2} & \cdots & \frac{\partial f_n}{\partial x_n} \end{bmatrix}$$

Suppose, $\delta = \mathbf{x} - \mathbf{x}^*$ and taking the derivative, we obtain $\dot{\delta} = \dot{\mathbf{x}}$ and since we are looking in the very small neighborhood of the fixed point, δ will be infinitesimal. So only the first two terms of the (1.9) are significant. Now, we have to analyze how the trajectories behave near the fixed point, i.e. whether the fixed point is *stable* or *unstable*. So, now we have

$$\dot{\delta} = \mathbf{J}^* \delta \tag{1.10}$$

where $\mathbf{J}^*$ is the Jacobian evaluated at the fixed point $\mathbf{x}^*$. Now, since the matrix $\mathbf{J}^*$ is just the constant, the equation (1.10) is nothing but just the linear differential equation and the solutions of this type of equations can be written as the linear combination of $e^{\lambda_j t}$ where λ_j's are the set of eigenvalues of the Jacobian matrix.

Now, the complex part of the eigenvalue will only contribute to an oscillatory component of the solution. So, just the real part matters for analyzing the stability of the fixed point. Now, if the $Re(\lambda_j) > 0$ then the $e^{\lambda_j t}$ will grow in time.

So, to conclude we see that a fixed point $\mathbf{x}^*$ of (1.8) is stable if all the eigenvalues of $\mathbf{J}^*$ have the negative real part and the fixed point is unstable if at least one of the eigenvalue has a positive real part. We will use this analysis in chapter 2(2.6).

Chapter 2

Analysis of Stuart Landau Oscillator

2.1 Introduction to Landau-Stuart Oscillator

Consider N number of Landau-Stuart (LS) oscillators interacting via mean-field[12] diffusive coupling.

$$\dot{Z} = (1 + i\omega_i - |Z_i|^2)Z_i + \epsilon(q\bar{Z} - Re(Z_i)) \tag{2.1}$$

The equation (2.1)[1] represents the mathematical model of LS Oscillator, where $i = 1, \ldots, N$; $\bar{Z}=\frac{1}{N}\Sigma_{i=1}^{N} Re(Z_i)$ is the mean-field of the coupled oscillator, $Z_i = x_i + jy_i$. The ϵ is the coupling strength, and q is a control parameter which determines the density of the mean-field ($0 \leq q \leq 1$); As $q \to 0$ the effect of the mean-field coupling decreases which suppresses the oscillations of the coupled system. When $q = 0$ there is no interaction and as a result system behaves as an uncoupled system with self-feedback, where $q = 1$ represents the maximum mean-field interaction.

We analyzed the system for $N = 2$ case. We will describe the analysis in the subsequent section in the following manner: First, the linear stability analysis of the LS oscillator along with the environment. Second, Stability analysis of the coupled LS oscillators with the variation in coupling strength. Following is the schematic diagram of the network with which we worked.

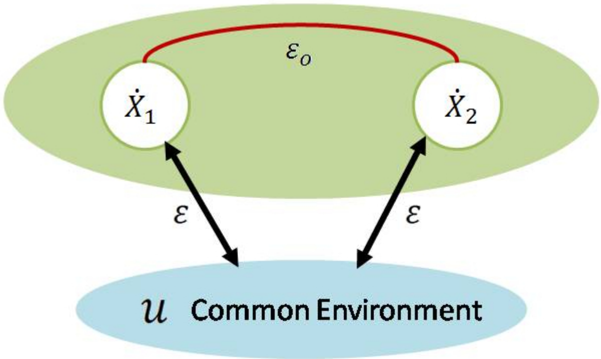

Figure 2.1: schematic diagram; $\dot{X}_1$ and $\dot{X}_2$ are two LS oscillators with coupling strength ϵ_0 and u a common environment coupled with oscillators with strength ϵ

2.2 Linear Stability Analysis

Consider the 2 LS oscillators with an environment, we analyzed the stability of the steady state. We write the variational form by linearizing (2.1) as

$$\dot{\eta_1} = f'(X_1)\eta_1 + \epsilon_0[\frac{q(\eta_1+\eta_2)}{2} - \eta_1] + \epsilon u \tag{2.2a}$$

$$\dot{\eta_2} = f'(X_2)\eta_2 + \epsilon_0[\frac{q(\eta_1+\eta_2)}{2} - \eta_2] + \epsilon u \tag{2.2b}$$

$$\dot{\eta_3} = -ku + \frac{\epsilon(\eta_1+\eta_2)}{2} \tag{2.2c}$$

Assuming that the time averaged value of $f'(X_1)$ and $f'(X_2)$ are approximately the same. We will replace it by effective constant value ζ.This type of approximation was used in [9][12] Also, in this approximation we will treat η_1, η_2 as the scalars. Therefore the Jacobian matrix of the (2.2) is

$$J_9(\eta_1,\eta_2,u) = \begin{pmatrix} \epsilon_0(\frac{q}{2}-1)_\zeta & \frac{q\epsilon_0}{2} & \epsilon \\ \frac{q\epsilon_0}{2} & \epsilon_0(\frac{q}{2}-1)_\zeta & \epsilon \\ \frac{\epsilon}{2} & \frac{\epsilon}{2} & -k \end{pmatrix} \tag{2.3}$$

The characteristic equation of the Jacobian matrix(J_9)(2.3) is given by:

$$(\epsilon_0 + \lambda - \zeta)(\epsilon^2 + (\zeta + \epsilon_0(q-1) - \lambda)(k+\lambda)) = 0 \tag{2.4}$$

The eigenvalues of this (2.4) are as follows:

$$\lambda_1 = \zeta - \epsilon_0 \tag{2.5a}$$
$$\lambda_{2,3} = \frac{1}{2}(\zeta + \epsilon_0(q-1) - k \pm (\sqrt[2]{4\epsilon^2 + (k + \epsilon_0(q-1) + \zeta)^2})) \tag{2.5b}$$

A coupled system goes to the stable steady state if the $Re(\lambda)$ is negative. So, we can say that for the transition from an unstable steady state to stable steady state is

$$\zeta - \epsilon_0 = 0 \tag{2.6a}$$
$$\frac{1}{2}(\zeta + \epsilon_0(q-1) - k \pm (\sqrt[2]{4\epsilon^2 + (k + \epsilon_0(q-1) + \zeta)^2})) = 0 \tag{2.6b}$$

This analysis we will be used for the analytical calculations done further.

2.3 Analysis of LS oscillator

Using the logic of section 4, we will write the model(given by (2.1)) in the Cartesian coordinate system with each oscillator as the function $f(x, y)$ and oscillators will be interacting with the environment u.

$$\dot{x}_1 = [1 - (x_1^2 + y_1^2)]x_1 - \omega_1 y_1 + \epsilon_0(q\bar{x} - x_1) \tag{2.7a}$$
$$\dot{x}_2 = [1 - (x_2^2 + y_2^2)]x_2 - \omega_2 y_2 + \epsilon_0(q\bar{x} - x_2) \tag{2.7b}$$
$$\dot{y}_1 = [1 - (x_1^2 + y_1^2)]y_1 + \omega_1 x_1 + \epsilon u \tag{2.7c}$$
$$\dot{y}_2 = [1 - (x_2^2 + y_2^2)]y_2 + \omega_2 x_2 + \epsilon u \tag{2.7d}$$
$$\dot{u} = -ku + \frac{\epsilon(y_1 + y_2)}{2} \tag{2.7e}$$

where $\bar{x} = \dfrac{x_1 + x_2}{2}$, ϵ_0 is a coupling strength between the two oscillators and ϵ is the coupling strength between the oscillator and the environment.
The Jacobian of the system given by (2.7) is $J(x_1, x_2, y_1, y_2, u)$:

$$\begin{pmatrix} \epsilon(\frac{q}{2} - 1) - 3x_1^2 - y_1^2 + 1 & \frac{\epsilon_0 q}{2} & -\omega - 2x_1y_1 & 0 & 0 \\ \frac{\epsilon_0 q}{2} & \epsilon_0(\frac{q}{2} - 1) - 3x_2^2 - y_2^2 + 1 & 0 & -\omega - 2x_2y_2 & 0 \\ \omega - 2x_1y_1 & 0 & -x_1^2 - 3y_1^2 + 1 & 0 & \epsilon \\ 0 & \omega - 2x_2y_2 & 0 & -x_2^2 - 3y_2^2 + 1 & \epsilon \\ 0 & 0 & \frac{\epsilon}{2} & \frac{\epsilon}{2} & -k \end{pmatrix} \tag{2.8}$$

The system has the following fixed points[13][1]:

1. Trivial fixed points :- $=(x_1^*, y_1^*, x_2^*, y_2^*, u^*)$=(0,0,0,0,0)
2. Inhomogeneous steady state, F_{IHSS}= $(x_1^*, y_1^*, x_2^*, y_2^*, u^*) = (a_1, b_1, -a_1, -b_1, 0)$
3. Non-trivial Homogeneous steady state = F_{HSS}= $(x_1^*, y_1^*, x_2^*, y_2^*, u^*) = (a_2, b_2, a_2, b_2, \frac{\epsilon b_2}{k})$

We will look at the analysis of Inhomogeneous and Homogeneous steady state in the subsequent sections. For further calculations, we're interested in the $\lambda - \epsilon$ plane and for that, we will fix some values of the variables used in equations (2.7) as follows:-

Variables	Value
k	1
ϵ_0	6
q	0.4

2.4 Results

2.4.1 Inhomogeneous Steady State

We substituted the steady state conditions given above in the equation (2.7) and will solve for a_1 and b_1.

$$[1-(a_1^2+b_1^2)]a_1 - \omega_1 b_1 - \epsilon_0 a_1 = 0 \tag{2.9a}$$
$$-[1-(a_1^2+b_1^2)]a_1 + \omega_2 b_1 + \epsilon_0 a_1 = 0 \tag{2.9b}$$
$$[1-(a_1^2+b_1^2)]b_1 + \omega_1 a_1 + \epsilon u = 0 \tag{2.9c}$$
$$-[1-(a_1^2+b_1^2)]b_1 - \omega_2 a_1 + \epsilon u = 0 \tag{2.9d}$$

By solving equations, (2.9a) and (2.9b), we get $\omega_1 = \omega_2$. For simplicity, let's assume $\omega_1 = \omega_2 = \omega$. We did further analysis at $\omega = 2$.
Further, solving and substituting the values we get the following equations:

$$[1-(a_1^2+b_1^2)]a_1 - 2b_1 - 6a_1 = 0 \tag{2.10a}$$
$$[1-(a_1^2+b_1^2)]b_1 + 2a_1 = 0 \tag{2.10b}$$

After solving equations(2.9), we got following values of a_1 and b_1.

a_1	b_1
-0.174	0.45
0.174	-0.45
-1.92ι	0.73ι
1.92ι	-0.73ι

We substituted the real values of a_1 and b_1 in equation (2.8) and calculated the characteristic equation for $a_1 = -0.174$ and $b_1 = 0.45$ which is as follow:

$$-5.93\epsilon^2+\lambda^5+8.45\lambda^4+\lambda^3(-\lambda^2+24.87)+\lambda^2(-7.81\epsilon^2+37.02)-\lambda(16.28\epsilon^2-25.6)+6.001 \tag{2.11}$$

Now, we varied the ϵ(the coupling strength between the oscillator and the environment) in a range of 0 to 2 and analyzed the variation of eigenvalues with the ϵ.

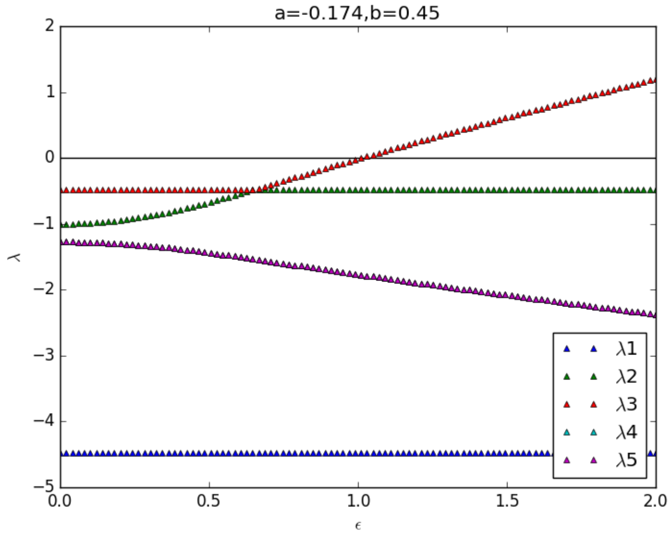

Figure 2.2: Distribution of λ s with ϵ

As, we, can see that λ_3 crosses the positive y-axis at ϵ ≈1. So, we analyzed the $Re(\lambda)$. For a steady state to be stable the $Re(\lambda) < 0$.

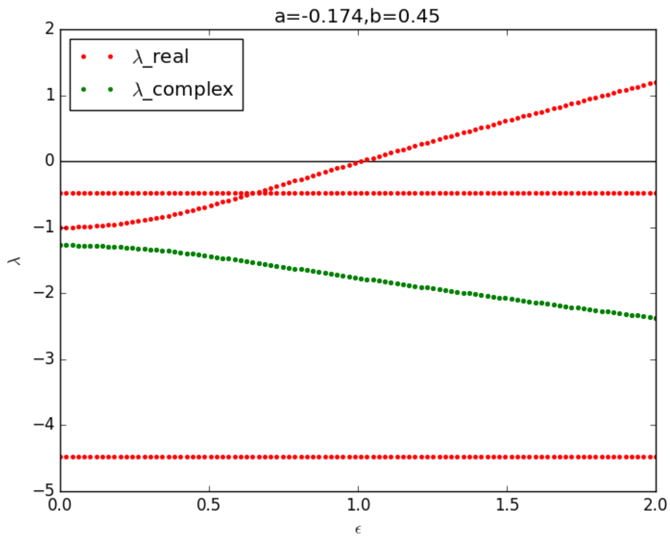

Figure 2.3: Distribution of $Re(\lambda)$ and $Im(\lambda)$ with ϵ

Here, we can see it clearly that the steady state is stable below ϵ ≈1 and above that it becomes unstable.

2.4.2 Homogeneous Steady State

We substituted the steady state conditions given above in the equations(2.7) and will solve for a_2 and b_2.

$$[1-(a_2^2+b_2^2)]a_2 - \omega_1 b_2 + \epsilon_0(qa_2 - a_2) = 0 \tag{2.12a}$$
$$[1-(a_2^2+b_2^2)]a_2 - \omega_2 b_2 + \epsilon_0(qa_2 - a_2) = 0 \tag{2.12b}$$
$$[1-(a_2^2+b_2^2)]b_2 + \omega_1 a_2 + \epsilon u = 0 \tag{2.12c}$$
$$[1-(a_2^2+b_2^2)]b_2 + \omega_2 a_2 + \epsilon u = 0 \tag{2.12d}$$
$$-ku + \epsilon b_2 = 0 \tag{2.12e}$$

By solving equations,(2.12c) and (2.12d), we get $\omega_1 = \omega_2$. For simplicity, let's assume $\omega_1 = \omega_2 = \omega$. We did further analysis at $\omega = 2$.
Further, solving and substituting the values we get the following equations:

$$[1-(a_2^2+b_2^2)]a_2 - 2b_2 - 3.6a_2 = 0 \tag{2.13a}$$
$$[1-(a_2^2+b_2^2)]b_2 + 2a_2 + b_2\epsilon^2 = 0 \tag{2.13b}$$

Since, a_2 and b_2 are dependent on ϵ, we, didn't get any specific values of a_2 and b_2. Using the varying values of the steady state with ϵ varying from 0 to 2. We analyzed the variation of the eigenvalues with ϵ.

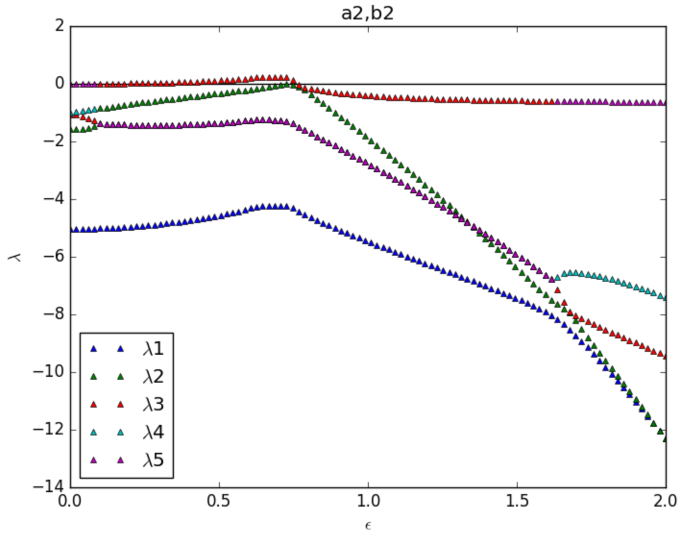

Figure 2.4: Distribution of λ s with ϵ

As we can see that $\epsilon \approx 0.67$ all the eigenvalues become negative. Then, we checked whether the real part of the eigenvalues is negative for the whole range of ϵ or not.

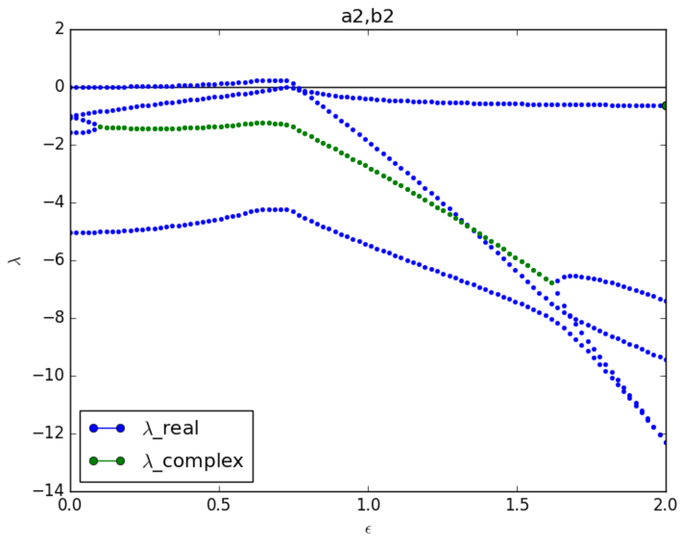

Figure 2.5: Distribution of $Re(\lambda)$ and $Im(\lambda)$ with ϵ

As we can see clearly that the $Re(\lambda)$ is above x-axis. So, after $\epsilon \approx 0.67$ $Re(\lambda)$ becomes negative and remains negative. So, that implies the system is stable after $\epsilon \approx 0.67$.

2.5 Discussion

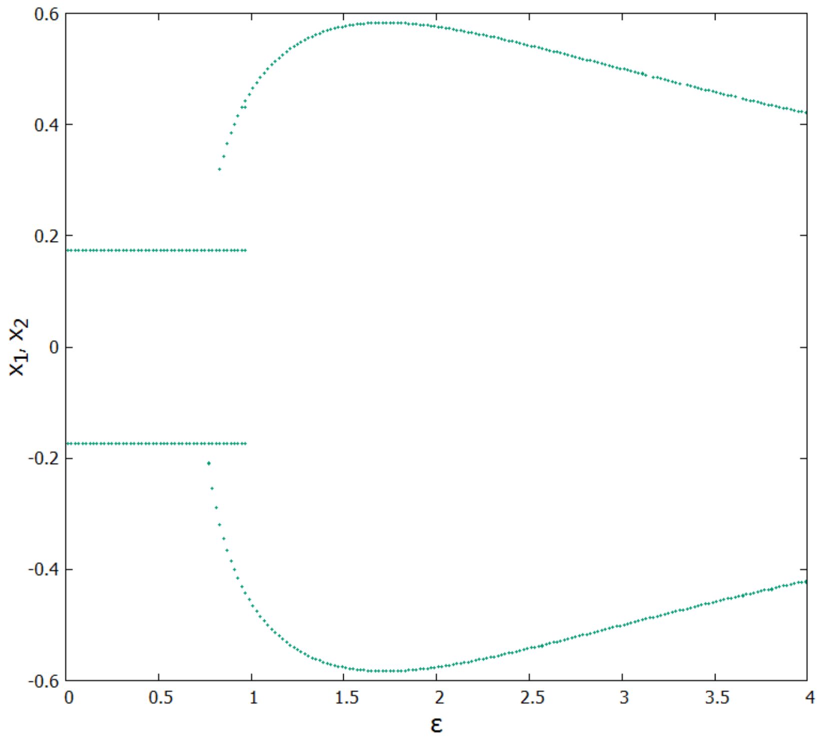

Figure 2.6: Two $[N = 2]$ environmentally coupled oscillators with ϵ

The numerical result of the steady state of two environmentally coupled oscillators presented in Figure2.6[16] solved using the RK-4 method with initial conditions between $[-1, 1]$ for $x_{i,j}$ and $[0, 1]$ for u. The region $\epsilon \leq 1$ is called the **OD** state which is referred here as the Inhomogeneous Steady State[16]. Also, the region $\epsilon \geq 0.7$ is called an **AD** which is referred here as the Homogeneous Steady State[16]. Also, in the region between $0.7 \leq \epsilon \leq 1$ the network is bistable.

In our, analytical result we can see that when $\epsilon \approx 0.7$ in the eigenvalue (IHSS figure) starts tending towards the positive x-axis and in HSS figure we can see that the eigenvalue crosses the positive y-axis at $\epsilon \approx 0.7$ only. So, the values obtained from the analytical analysis are consistent with the numerical result[16] obtained.

Chapter 3

Analysis of the Multiplex Network

3.1 Introduction

In this chapter, we studied the synchronous state of the network which had the multilayer construction. The networks considered in this study is time static, i.e. the links between the nodes doesn't vary with the time. Developments in recent past in the study of fields of the multi-layered network, a *multiplex network* provides the important framework for the realistic description of the large number of system[2, 6]. In this kind of network, the processes occurring in one network may have an effect on the other network as well, which is taken into account and the way in which one layer is coupled/connected(to the other nodes)may differ from each other. This has also helped us in understanding the outcomes of interconnections in a different complex system, like epidemic spreading processes[11, 3, 10, 5], congestion in traffic[7] and air transportation network[4], etc.

Usually, the networks consist of two or more layers. In our study, we took two layer network, in which the topology of both the layers where different. In a multiplex network, we, generally study two types of interaction: *Intra-layer* and *Inter-layer*. In intra-layer, we study the interaction between the nodes in the same layer and in the latter one we study the interaction between the replica nodes of the different layer[8].

The first layer will be denoted by $\mathbf{X}$ and the second one by $\mathbf{Y}$. The topology for the layer $\mathbf{X}$ is that of regular ring topology where each node is connected to $2k$ nearest neighbor i.e the i^{th} node is connected to $(i-k)^{th}$ and $(i+k)^{th}$ node and the topology for the layer **Y** is that of a *small-world network*. The small-world network is constructed by Watts-Strogatz procedure as given in[15].

Def:-The small-world network is a network in which the shortest distance between the nodes grows slowly. Shortest distance is defined as the minimum number of edges that should be traversed from one node to the destination node. In a small-world network, if the shortest distance between two randomly chosen node is ℓ and the number of nodes in Network is N then

$$\ell \propto logN \tag{3.1}$$

The small-world network is characterized by two properties:

- Small average shortest path length which is given by (3.1).
- Large clustering coefficient.

Def:- Let the number of node in a network(G) be N. The clustering coefficient(CC) of G is given by

$$CC(G) = \frac{1}{N} \sum_{Node=1}^{N} CC(Node) \tag{3.2}$$

Let V be a node and K_V be the degree of the node V, i.e. to how many nodes, node V is connected. Let N_V be the number of links between the neighbors of V. Then the $CC(V)$ is given by

$$CC(V) = \frac{2N_V}{K_V(K_V - 1)} \tag{3.3}$$

So, for the layer Y, we start with N nodes with regular ring topology where each node is connected to the $2k$ neighbors, k on each side. Then with probability p, we reconnect all the edges to vertices chosen uniformly at random.

3.1.1 Logistic Maps

The logistic map is defined by:

$$x_{n+1} = rx_n(1 - x_n) \tag{3.4}$$

Logistic map is the discrete equation for population growth model. It's a classic example of how complex and chaotic behavior can arise from simple non-linear equation.
x_n varies between 0 and 1. The control parameter r is restricted to $[0, 4]$ between which we see very interesting dynamics.

- When $r < 1$, the population will go extinct, i.e. $x_n \to 0$ as $n \to \infty$, no matter what was the initial population size.
- When $1 < r < 3$, the population will approach to steady state $(\frac{r-1}{r})$, independent of the initial population size.
- When $r > 3$, the population oscillates in two-period cycle till $r < 3.4$. Above that population oscillates between four-period cycle till $r < 3.5$. For higher values of r, we will see 8,16,32,$\cdots$ periods cycle. This is called period-doubling bifurcation, and chaotic behavior can be observed.

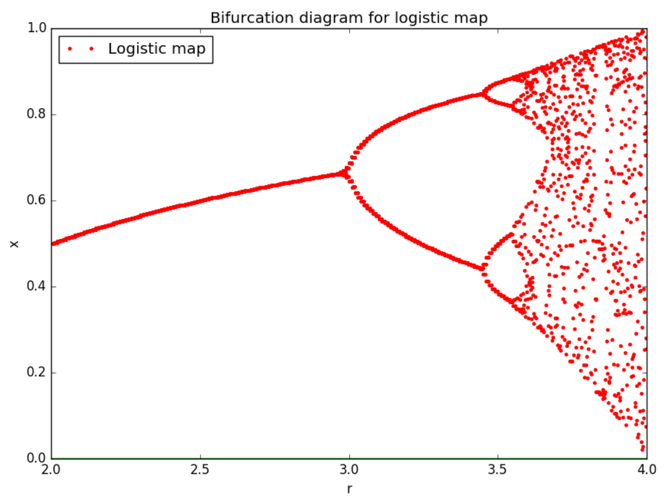

Figure 3.1: Period-doubling bifurcation in logistic map

3.1.2 Lyapunov Exponent

A Lyapunov exponent of any dynamical system characterizes the rate of separation between two very close trajectories. Positive Lyapunov exponent indicates that the system is chaotic because if you start with two initial conditions which are very close to each other, say x_0 and y_0=$x_0 + \delta$, where δ is infinitesimal. And we evolve them under the map, then the difference between the trajectories/two-time series given by $\delta_n = x_n - y_n$ diverges exponentially. The rate of divergence is given by

$$|\delta_n| = |\delta_0|\, e^{\lambda n} \tag{3.5}$$

where λ is called the **Lyapunov Exponent**.
Now, after rearranging equation(3.5), we get

$$\lambda = \lim_{n\to\infty} \frac{1}{n} ln\left|\frac{\delta_n}{\delta_0}\right| \tag{3.6}$$

Now, by definition we know,

$$\delta_n = f^n(x_0 + \delta_0) - f^n(x_0) \tag{3.7}$$

Substituting this in equation(3.6), we get

$$\lambda = \lim_{n\to\infty} \frac{1}{n} ln\left|\frac{f^n(x_0 + \delta_0) - f^n(x_0)}{\delta_0}\right| \tag{3.8}$$

For $\delta_0 \to 0$, the numerator inside the mod is just the derivative of f^n evaluated at $x = x_0$. So,

$$\lambda = \frac{1}{n} ln\left|\frac{df^n}{dx}\right|_{x=x_0} \tag{3.9}$$

Also,

$$f^n(x) = f(f(f(\cdots f(x)))) \tag{3.10}$$

So, by the chain rule

$$\left.\frac{df^n}{dx}\right|_{x=x_0} = \prod_{i=0}^{n-1} f'(x_i) \tag{3.11}$$

Hence, the formula for lyapunov exponent becomes,

$$\lambda = \frac{1}{n} ln \left| \prod_{i=0}^{n-1} f'(x_i) \right| = \frac{1}{n} \sum_{i=0}^{n-1} ln(|f'x_i|) \tag{3.12}$$

Lyapunov exponent contains an average over a trajectory, and for the stable fixed point the orbit turns out to be a fixed point. Hence, the contribution by the fixed point dominates the average and, we get

$$\lambda = ln|f'(x^*)| \tag{3.13}$$

By, using equation (3.13) we found out the lyapunov exponent for the logistic equation and to see whether it shows chaotic behavior or not.

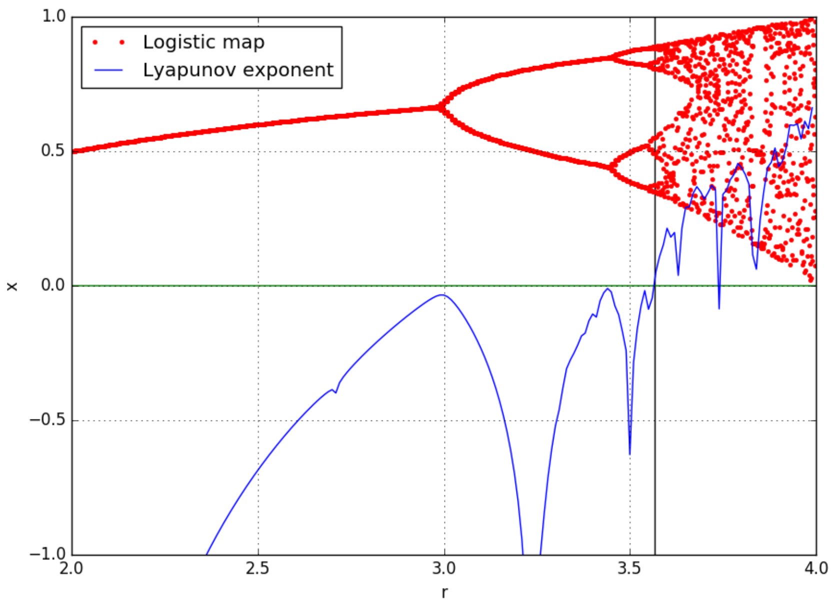

Figure 3.2: Bifurcation in logistic map and the trajectory of the lyapunov exponent

3.2 Dynamics of the Multiplex Network of Logistic Map

3.2.1 Model

We have considered two layers defined by the topology given above. Each layer has N nodes of a single dimension. So, the state of the layers is given by $\mathbf{X}=\{\mathbf{x_1},\mathbf{x_2},\cdots,\mathbf{x_N}\}$ and $\mathbf{Y}=\{\mathbf{y_1},\mathbf{y_2},\cdots,\mathbf{y_N}\}$ where $\mathbf{x_i}$ and $\mathbf{y_i} \in \mathbb{R}\ \forall\ i$.

The model under study is described by the following system of equations:

$$\mathbf{x}_i^{t+1} = f_i^t + \frac{\epsilon}{2k}\sum_{j=1}^{N}\mathcal{A}^1_{i,j}(f_j^t - f_i^t) + \gamma F_i^t \tag{3.14}$$

$$\mathbf{y}_i^{t+1} = g_i^t + \frac{\epsilon}{2k}\sum_{j=1}^{N}\mathcal{A}^2_{i,j}(g_j^t - g_i^t) + \gamma G_i^t \tag{3.15}$$

where x_i^t and y_i^t are the real dynamical variable of the coupled ensemble, N is the total number of oscillator in each sub-network, t is the discrete time variable.
In our study, both the sub-network are defined by the logistic map.

$$f_i^t = \alpha_1 x_i^t(1 - x_i^t) \tag{3.16}$$

$$g_i^t = \alpha_2 y_i^t(1 - y_i^t) \tag{3.17}$$

with different control parameters α_1 and α_2. ϵ is the intra-layer coupling strength within the sub-network and γ signifies the inter-layer coupling strength between the sub-network.

$$F_i^t = (g_i^t - f_i^t) \tag{3.18}$$

$$G_i^t = (f_i^t - g_i^t) \tag{3.19}$$

The functions in the equations, (3.18) and (3.19) are the coupling functions between the sub-networks.
$\mathcal{A}^{1,2} = (\mathcal{A}^{1,2}_{i,j})_{N\mathrm{x}N}$ are the adjacent matrices which are defined as:

$$\mathcal{A}^{1,2}_{i,j} = \begin{cases} 1 & \text{if the } i^{th} \text{ and } j^{th} \text{ node are connected,} \\ 0 & \text{otherwise} \end{cases}$$

As we can see in figure 3.2 that for $r > 3.56$ the logistic map shows chaotic behavior. So, from there we choose the values of α_1 and α_2 for further study of the multiplex network. In this study we focused on two types of synchronization: intra-layer and inter-layer synchronization.

Def: Intra-layer synchronization is defined as the state of synchrony in which nodes within the layer evolve synchronously, independent of whether layers evolve coherently or not[8].

Def: Inter-layer Synchronization is defined as the state of synchrony where the layers are synchronized but, nodes within each layer may not be[8].

So, In our formulation, we have considered $N = 10$ and $k = 1$, with non-identical layers in the network and on each node we have the system as the logistic map which is defined by the equations,(3.16) and (3.17), $\alpha_1 = 3.7$ and $\alpha_2 = 3.85$. So, that the system is in the chaotic regime and the model formulation is given by equation(3.14) for layer $\mathbf{X}$ and by equation (3.15) for layer $\mathbf{Y}$.
We will study Intra-layer and Inter-layer synchronization in which emphasis will be to identify parameter regions for intra-layer and inter-layer synchronization, under variations of following parameters: Intra-layer and Inter-layer coupling strength,the probability of re-linking of the edges and the difference between α_1 and α_2.
Without loss of generalization, we will assume that the intra-layer strength is much more than the inter-layer strength, specifically $\epsilon = 3\gamma$. The Intra-layer synchronization is given by:

$$E_{intra} = \lim_{T\to\infty} \frac{1}{T} \int_0^T \sum_{j=2}^{N} \frac{\|x_j(t) - x_1(t)\|}{N-1} dt \tag{3.20}$$

and Interlayer synchronization is given by,

$$E_{inter} = \lim_{T\to\infty} \frac{1}{T} \int_0^T \sum_{j=2}^{N} \frac{\|\delta z_i(t)\|}{N-1} dt \tag{3.21}$$

where $\delta z_i(t)= x_i(t) - y_i(t)$ is the difference between the layer dynamics at the i^{th} node, $\|.\|$ is the Euclidean norm[].

3.3 Results

- Effect of varying number of nodes of each layer. Here $\alpha_1 = 3.7$ and $\alpha_2 = 3.85$ and the probability(p) of relinking in layer 2 is $p = 0.5$.

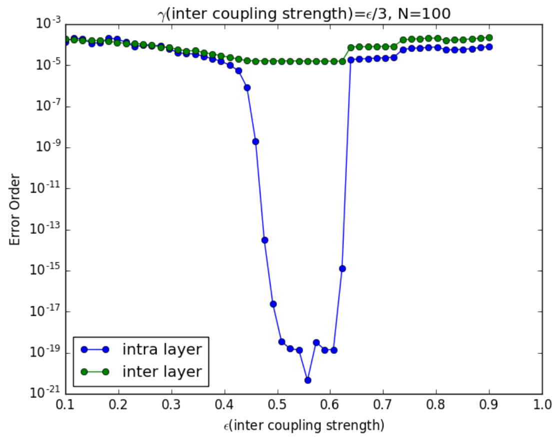

(a)

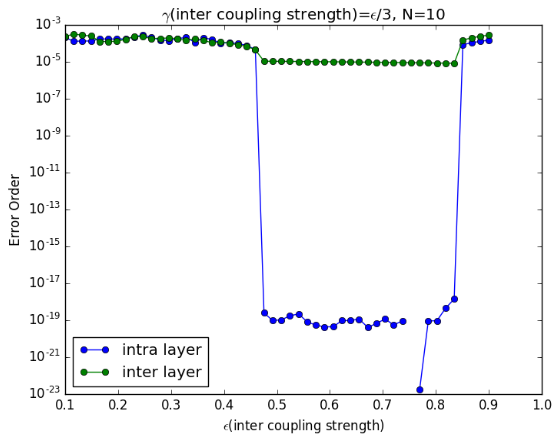

(b)

Figure 3.3: (a) 100 oscillators and (b) 10 oscillators (γ=$\epsilon/3$)

- Effect of varying $\Delta\alpha = \alpha_2 - \alpha_1$. Here also, $p = 0.5$ for layer Y and 10 nodes in each layer.

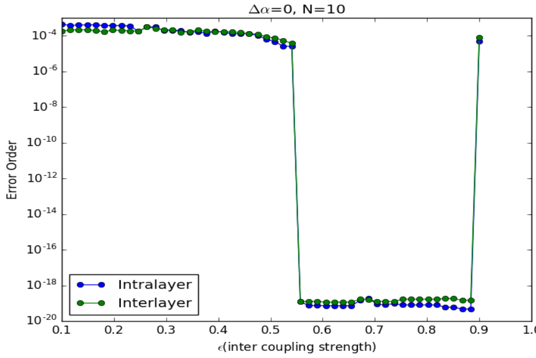

(a)

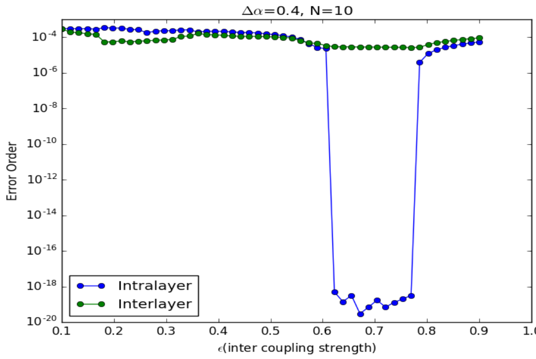

(b)

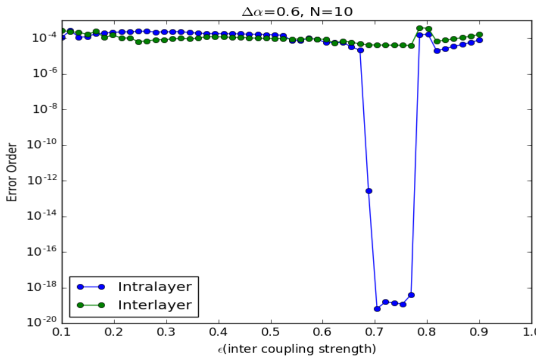

(c)

Figure 3.4: (a)$\Delta\alpha = 0(\alpha_1 = \alpha_2 = 3.7)$ (b)$\Delta\alpha = 0.4(\alpha_1 = 3.5\ \alpha_2 = 3.9)$ (c)$\Delta\alpha = 0.6(\alpha_1 = 3.4\ \alpha_2 = 4)$

- Effect of varying both ϵ and γ with fixed $\alpha_1 = 3.7$ and $\alpha_2 = 3.85$

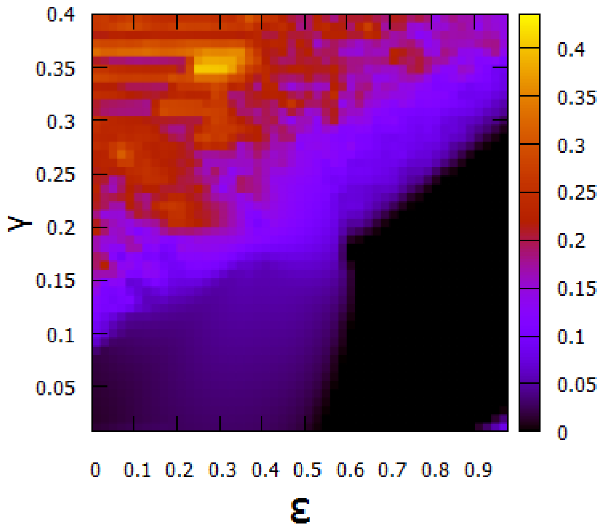

(a)

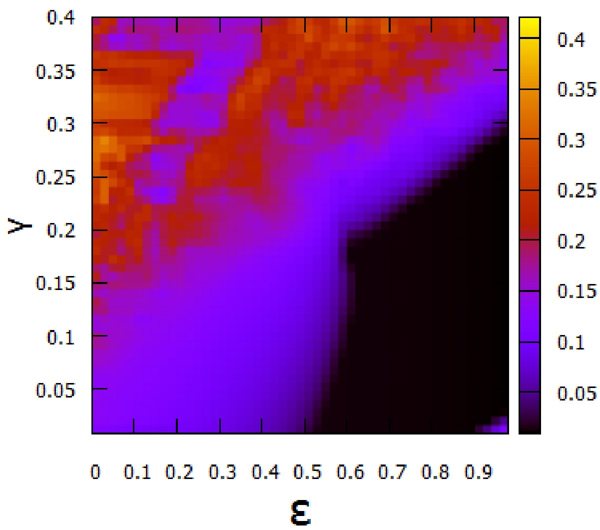

(b)

Figure 3.5: (a) Intra-layer and (b) Inter-layer Synchronization Error for varying the intra-layer and inter-layer coupling strength

- In this we observed the effect on the synchronization parameter space by varying the probability of the layer Y.

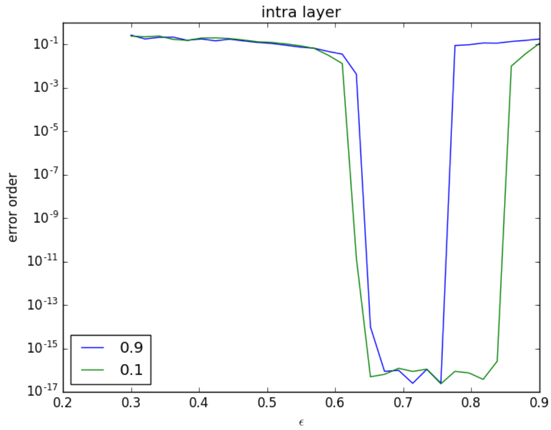

(a)

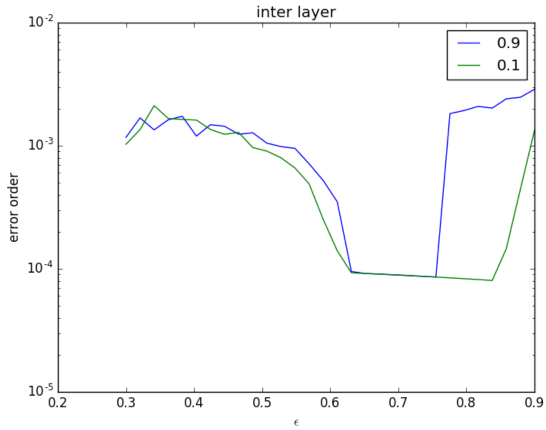

(b)

Figure 3.6: (a) Intra-layer and (b) Inter-layer Synchronization Error for different probabilities

- Snapshot of representative spatial profiles for various ϵ for both the layer. $\alpha_1 = 3.7$,$\alpha_2 = 3.85$,$p = 0.5$ and $\gamma = \epsilon/3$

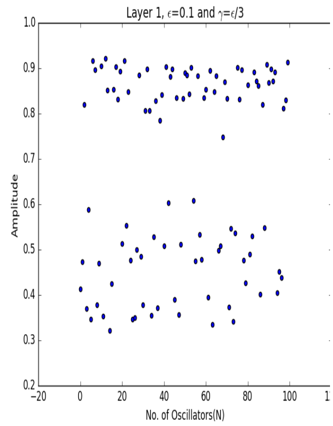

(a)

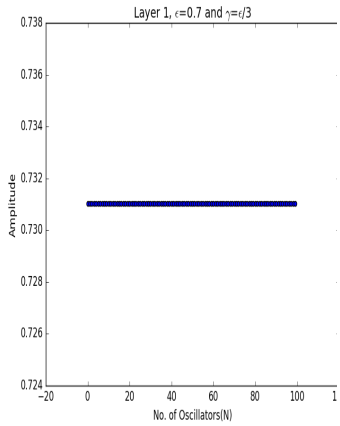

(b)

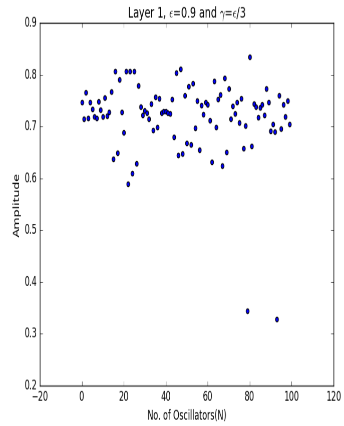

(c)

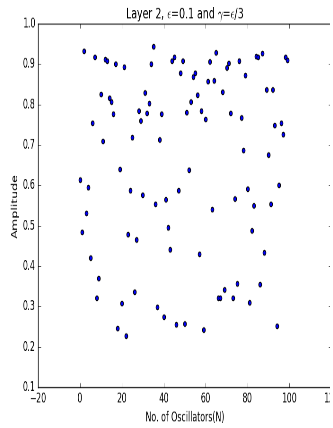

(d)

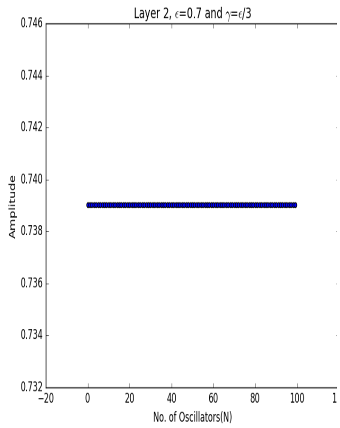

(e)

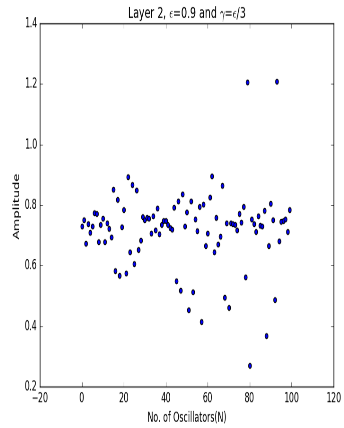

(f)

Figure 3.7: Layer X (top) and layer Y (bottom); Columns (L to R): $\epsilon = 0.1$, $\epsilon = 0.7$ (complete synchronization) and $\epsilon = 0.9$

3.4 Conclusion

- Intra-layer and inter-layer synchronization regions in the parameter space of inter-layer and intra-layer coupling strengths were identified.
- We observed that inter-layer synchronization was drastically affected by parameter mismatch in the nodal dynamics of the layers.
- For large coupling strength ϵ, synchronization within layers, as well as between networks can be achieved.
- Although the edge re-linking probability has a slight effect on the synchronization regions, compared to the other parameters, it does not affect the synchronization regions significantly.
- In the parameter region $0.5 \leq \epsilon \leq 0.9$ and $0 \leq \gamma \leq 0.3$ we achieved complete synchronization.
- Increase in number of nodes across both layers decreases the range in parameter space yielding complete synchronization.
- In future, we will try to extend this analysis to time-varying networks.

Summary

To summarize, we first studied fundamental properties of dynamical systems, classification of fixed points and linear stability analysis. We also generalized these concepts to higher dimensional systems.

Next, we studied a specific illustrative example of a group of limit cycle oscillators coupled via a common external environment. We found out analytically the transition of Inhomogeneous steady states (IHSS) to Homogeneous steady states (HSS) in the parameter space of the coupling strength of the oscillator and the common environment. We also found the parameter region in which both IHSS and HSS are stable, and the results were compatible with existing results from numerical simulations.

Further, we studied multiplex networks of logistic maps. In particular, we focused on intra-layer and inter-layer synchronization and identified the region where synchronization is achieved, in the parameter space of intra-layer and inter-layer coupling strengths. Lastly, the effect of various parameters on intra-layer and inter-layer synchronization was also investigated.

Bibliography

[1] T. Banerjee and D. Ghosh, *Transition from amplitude to oscillation death under mean-field diffusive coupling*, PHYSICAL REVIEW E, 89 (2014).

[2] S. Boccaletti, G. Bianconi, R. Criado, C. I. del Genio, J. Gomez-Gardenes, M. Romance, I. Sendina-Nadal, Z. Wang, and M. Zanin, *The structure and dynamics of multilayer networks*, Phys. Rep., 544 (2014).

[3] C. Buono, L. G. Alvarez-Zuzek, P. A. Macri, and L. A. Braunstein, *Epidemics in partially overlapped multiplex networks*, PLOS ONE, 9 (2014).

[4] A. Cardillo, M. Zanin, J. Gomez-Gardenes, M. Romance, A. G. del Amo, and S. Boccaletti, *Modeling the multi-layer nature of the european air transport network: Resilience and passengers re-scheduling under random failures*, The European Physical Journal Special Topics, 215 (2013), pp. 23–33.

[5] C. Granell, S. Gomez, and A. Arenas, *Dynamical interplay between awareness and epidemic spreading in multiplex networks*, Phys. Rev. Lett., 111 (2013).

[6] M. Kivela, A. Arenas, M. Barthelemy, J. P. Gleeson, Y. Moreno, and M. A. Porter, *Multilayer networks*, Journal of Complex Networks, 2 (2014), pp. 203–271.

[7] R. G. Morris and M. Barthelemy, *Transport on coupled spatial networks*, Phys. Rev. Lett., 109 (2012).

[8] S. Rakshit, S. Majhi, B. Bera, S. Sinha, and D. Ghosh, *Time-varying multiplex network: Intralayer and interlayer synchronization*, PHYSICAL REVIEW E, 96 (2017).

[9] V. Resmi, G. Ambika, and R. E. Amritkar, *Synchronized states in chaotic systems coupled indirectly through dynamic environment*, Phys Rev E, 81 (2010).

[10] J. Sanz, C. Y. Xia, S. Meloni, and Y. Moreno, *Dynamics of interacting diseases*, Physical Review X, 4 (2014).

[11] A. Saumell-Mendiola, M. Angeles Serrano, and M. Boguna, *Epidemic spreading on interconnected networks*, Phys. Rev. E, 86 (2012).

[12] A. Sharma and M. D Shrimali, *Amplitude death with mean-field diffusion*, PHYSICAL REVIEW E, 85 (2012).

[13] M. Soumen, B. Bidesh, B. Sourav, and G. Dibakar, *Restoration of oscillation in network of oscillators in presence of direct and indirect interactions*, Physics Letters A, 35 (2016), pp. 1–8.

[14] S. H. Strogatz, *Nonlinear Dynamics and Chaos*, Perseus Books, 1994.

[15] D. J. Watts and S. H. Strogatz, *Collective dynamics of small-world networks*, Nature(London), 393 (1998), pp. 440–442.

[16] M. Yadav, A. Sharma, M. D. Shrimali, and S. Sinha, *Revival of oscillations via common environment*, Nonlinear Dynamics, 91 (2018), pp. 2219–2225.